Thermodynamic Model for the Analysis of Calorimetric Data of Oligomeric Proteins

Inés Burgos,*,† Sergio A. Dassie,‡ and Gerardo D. Fidelio†

Departamento de Química Biológica, Centro de Investigaciones en Química Biológica and Departamento de Fisicoquímica, Instituto de Investigaciones en Fisicoquímica de Córdoba (CONICET), Facultad de Ciencias Químicas, Universidad Nacional de Córdoba, Argentina

Received: May 20, 2008; Revised Manuscript Received: July 24, 2008

The thermodynamic parameters for the process of protein unfolding can be obtained through differential scanning calorimetry. However, the unfolding process may not be a two-state one. Between the native and the unfolded state, there may be association or dissociation processes or the formation of an intermediate state. As a consequence of this, the precise interpretation of the calorimetric data should be done with a specific thermodynamic model. In this work, we present two general models for the unfolding process of an oligomeric protein: $N_n \rightleftharpoons nN \rightleftharpoons nD$ (model A) and $N_n \rightleftharpoons I_n \rightleftharpoons nD$ (model B). In model A, the first step represents the dissociation of the oligomer into the monomeric native species, and the second step represents the denaturation process. In model B, the first step represents the conformational change of the oligomer, and the second step represents the dissociation of this species with the concomitant unfolding process. A canonical ensemble was employed to describe these systems, by considering that the total protein concentration remains constant. In the present work, we show and analyze the behavior of these systems in different conditions and how this analysis could help with the identification of the unfolding mechanism experimentally observed.

1. Introduction

Oligomeric proteins are extensively present in biology. Many enzymatic and binding proteins are only active when they assemble into dimers, tetramers, or even higher oligomeric states. It is also known that they may modulate their enzymatic or receptor activity by their degree of oligomerization, either through a structural pattern or by cooperative interactions.[1−3] Protein oligomers were also postulated to be involved in the mechanism of some neurodegenerative diseases,[4] and recently, there have been reported works which point out that small and reversible oligomers would be the toxic agents which cause major damage.[5]

The oligomerization process, as all the equilibrium reactions, can be induced or affected by several environmental conditions such as temperature, pH, ionic strength, and, specifically, total protein concentration. Changes on any of these factors may tend to dissociate or associate the oligomer depending on molecular and thermodynamic aspects. The thermodynamics that governs the process of oligomerization has been little studied through calorimetric techniques. Takahashi and Sturtevant studied the *Streptomices* subtilisin inhibitor, a dimeric protein, employing differential scanning calorimetry (DSC).[6] The thermodynamic parameters obtained from the protein thermal unfolding, with DSC, help understand the physics of protein oligomerization. They proposed that the unfolding of wild type subtilisin inhibitor is a two-state process in which the native dimeric protein would unfold and dissociate, in a single step, into unfolded monomeric proteins. Sturtervant's group also studied the mutant forms of *Streptomices* subtilisin inhibitor, which had punctual aminoacidic replacements, and they observed that the unfolding of some of them was not a two-state process, as a consequence of having an intermediate state. The experimental DSC traces were fitted by considering, in some cases, a conformational oligomeric intermediate state[7] and, in other cases, the dissociation of the dimer into the native monomers coupled to the unfolding process with a semiempiric approach.[8] However, a formal thermodynamic model for oligomeric proteins was not developed until the work presented by Rösgen and Hinz.[9] In this work, they obtained the thermodynamic equations which describe the two-state transition of a native oligomer into the denatured monomers, $N_n \rightleftharpoons nD$. These authors observed that, unlike the model developed previously for protein transitions with a stoichiometry 1:1,[10] in the model for the unfolding of oligomeric proteins, the enthalpy is not proportional to the fraction of the unfolded protein. They used a thermodynamic statistic approach by considering the protein system as a canonical ensemble.

In the present work, we develop a thermodynamic model with two variants which describe more complex oligomeric systems. With these models, we are able to simulate the experimental calorimetric unfolding of oligomeric protein complexes described previously,[7,8] and it is possible to predict the stability and thermodynamic behavior of the system.

2. Theory

In general, the heat capacity of a system relative to a reference state as a function of temperature (T), for pressure (P) constant, is derived from the expression of the enthalpy of the system relative to the enthalpy of the reference state, RS:

$$C_P - C_{P,\mathrm{RS}} = \frac{\mathrm{d}(H - H_{RS})}{\mathrm{d}T} \tag{1}$$

To obtain the analytical expression of the enthalpy, it is necessary to know the relative partition function of the system (Q) and its partial derivative respect to T for total number of particles constant:

* Corresponding author: E-mail: inesburgos@fcq.unc.edu.ar. Phone: 54 351 4334171. Fax: 54 351 4334074.
† Departamento de Química Biológica.
‡ Departamento de Fisicoquímica.

10.1021/jp804465c CCC: $40.75
Published on Web 10/22/2008

$$H - H_{RS} = k_B T^2 \frac{\partial \ln Q}{\partial T}\bigg|_C \quad (2)$$

In Sections 2.1 and 2.2, the models for two different oligomeric protein systems are presented. For both cases, we considered the native monomeric species (N) as the reference state, and the total number of particles refers to the total protein monomer concentration (C).

2.1. Process of Oligomerization Coupled with Unfolding Equilibrium, Model A. We developed the equations which describe a protein system where the native protein monomer, N, is in equilibrium with the native n-oligomeric species, N_n, and the unfolded monomeric protein, D, according to the following reactions:

$$N \rightleftharpoons D \quad (I)$$

$$nN \rightleftharpoons N_n \quad (II)$$

The reactions I and II are characterized by their equilibrium constants:

$$K_D(T) = \frac{[D]}{[N]} \quad (3)$$

$$K_n(T) = \frac{[N_n]}{[N]^n} \quad (4)$$

By considering the total protein monomer concentration, the mass balance of the system can be expressed by

$$C = [N] + n[N_n] + [D] = [D]\left(\frac{1 + K_D(T)}{K_D(T)}\right) + \frac{nK_n(T)[D]^n}{(K_D(T))^n} \quad (5)$$

The relative partition function for the protein system, when assuming a canonical ensemble, can be written as a function of the species concentration.[9]

$$Q = \frac{[N] + [D] + n[N_n]}{[N]} = 1 + K_D(T) + \frac{nK_n(T)[D]^{(n-1)}}{(K_D(T))^{(n-1)}} = Q_N + Q_D + Q_{Nn} \quad (6)$$

Then, the analytical expression of the enthalpy of the protein system relative to the enthalpy of the native state can be obtained by taking the partial derivative of Q with respect to temperature, for total protein concentration constant:

$$H - H_N = k_B T^2 \frac{\partial \ln Q}{\partial T}\bigg|_C \quad (7)$$

The algebraic procedure employed to derive Q is explained in the Appendix section. Then, the analytical expression obtained for the enthalpy change is eq 8:

$$H - H_N = [\Delta H_D \alpha_D + \Delta H_n \alpha_{Nn}]\left[\frac{1}{1 + (n-1)\alpha_{Nn}}\right] \quad (8)$$

where $\alpha_i = Q_i/Q$.

2.2. Conformational Change Process Coupled with Dissociation-Unfolding Equilibrium, Model B. We also developed the model which describes a protein system where a nonnative protein oligomer, I_n, is in equilibrium with the native n-oligomeric species, N_n, and the unfolded monomeric protein, D, according to the following reactions.

$$I_n \rightleftharpoons nD \quad (III)$$

$$N_n \rightleftharpoons I_n \quad (IV)$$

The reactions III and IV are characterized by their equilibrium constants:

$$K_{ID}(T) = \frac{[D]^n}{[I_n]} \quad (9)$$

$$K_{In}(T) = \frac{[I_n]}{[N_n]} \quad (10)$$

The mass balance of the system, for total protein monomer concentration, can be expressed by:

$$C = n[I_n] + n[N_n] + [D] = \frac{n[D]^n}{K_{ID}(T)}\left(\frac{1 + K_{In}(T)}{K_{In}(T)}\right) + [D] \quad (11)$$

This is the relative partition function for the protein system, when assuming a canonical ensemble, written as a function of the species concentrations:

$$Q = \frac{n[N_n] + n[I_n] + [D]}{n[N_n]} = 1 + K_{In}(T) + \frac{K_{In}(T)K_{ID}(T)[D]^{(1-n)}}{n} = Q_{Nn} + Q_{In} + Q_D \quad (12)$$

Then, the analytical expression of the enthalpy of the protein system relative to the enthalpy of the native state can be obtained from Q, as it was stated in eq 7.

$$H - H_N = \Delta H_{In}\left[\frac{\alpha_{In} + \alpha_D + \alpha_D\alpha_{Nn}(1-n)}{n(\alpha_{Nn} + \alpha_{In}) + \alpha_D}\right] + \Delta H_{ID}\left[\frac{\alpha_D + (1-n)\alpha_D(\alpha_{In} + \alpha_{Nn})}{n(\alpha_{Nn} + \alpha_{In}) + \alpha_D}\right] \quad (13)$$

where $\alpha_i = Q_i/Q$.

ΔH_i for both eq 8 and eq 13 was assumed to have the following temperature dependence:

$$\Delta H_i = \Delta H_i^\circ + \Delta C_{P_i}(T - T_i) \quad (14)$$

where ΔH_i° is the enthalpy change for the reaction i at the reference temperature, T_i, and ΔC_{Pi} is the heat capacity difference between the final and initial state of each process. For this model, it is assumed that the ΔC_{Pi} value is temperature independent.

Finally, the heat capacity of the protein system with both models can be derived with respect to temperature, numerically or analytically, from the analytical expression of the enthalpy:

$$C_P - C_{P,N} = \frac{d(H - H_N)}{dT} \quad (15)$$

3. Results and Discussion

The results are presented in four subsections. Section 3.1 shows results obtained with model A for a protein dimer changing total protein concentration and the enthalpy of the dimerization process. Section 3.2 shows the effect of the oligomerization number on a protein system simulated with model A. Section 3.3 has some results of the total protein

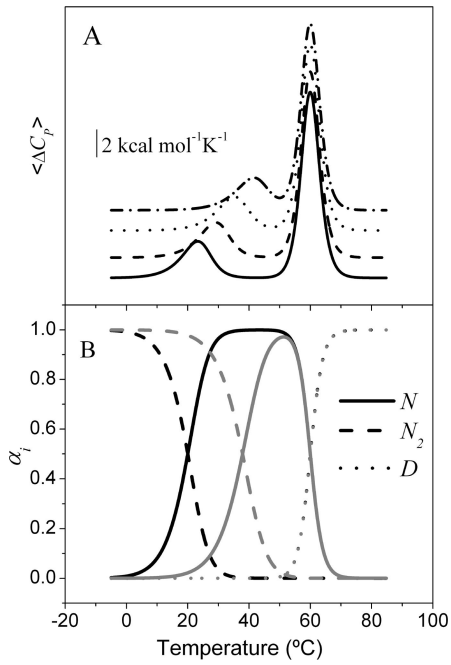

Figure 1. Effect of total protein concentration on the stability of a dimeric protein complex. (A) Simulated thermograms changing total protein concentration $C = 1 \times 10^{-7}$ M (solid line), 1×10^{-6} M (dashed line), 1×10^{-5} M (dotted line), 1×10^{-4} M (dashed-dotted line). (B) Species temperature-dependence profiles. Simulation parameters: $n = 2$, $T_d = 60$ °C, $\Delta H_d = 110$ kcal mol^{-1}, $\Delta C_P = 0$ kcal mol^{-1} K^{-1}, $K_n = 1 \times 10^7$ M^{-1}, $T_n = 20$ °C, $\Delta H_n = -70$ kcal mol^{-1} of dimer, $\Delta C_{Pn} = 0$ kcal mol^{-1} K^{-1}.

concentration and oligomerization number dependence on the stability of a protein system simulated with model B. Finally, Section 3.4 compares experimental results with simulated calorimetric profiles obtained with model B.

3.1. Results Obtained with Model A for a Protein Dimer.

3.1.1. Effect of Changing Total Protein Concentration on Simulated Calorimetric Profiles. The study of the effect of total protein monomer concentration, C, on protein stability is a typical experiment done when working with oligomeric proteins. Increasing C produces a stabilization of the oligomeric species with different consequences depending on the particular system. Figure 1 shows a representative case. Panel A shows biphasic endotherms at different C values. As C increases, the first transition progressively occurs at higher temperatures, whereas the second transition is not affected. Panel B shows the temperature dependence of the species profiles for the lowest and the highest protein concentration. It can be observed that the first transition is the heat uptake when the native dimer dissociates into the native monomers and the second transition is the unfolding of the native monomers. Both processes can be represented with the following global reaction:

$$N_2 \rightleftharpoons 2N \rightleftharpoons 2D \qquad (V)$$

When C increases, the dimer is stabilized, and the dissociation takes place at higher temperatures. The second process does not involve a change in the molecularity; therefore, it remains unaltered.

The same tendency is observed if the constant value of the dimerization reaction (K_n) is changed (data presented in the Supporting Information, Figure S1). The equilibrium constant value for a given process at any temperature cannot be modified. However, with an experimental approach, the apparent equilibrium constant can be modified by changing the solution conditions such as the pH or ionic strength. We analyzed the consequences of modifying the equilibrium constant value of the dimerization process on protein stability with K_n ranging from 1×10^3 M^{-1} to 1×10^7 M^{-1} (data presented in the Supporting Information, Figure S1). The temperature at which the heat capacity of the first transition has it maximum value, T_{m1}, is higher for larger K_n values. On the contrary, the T_m value of the second transition remains constant. Larger K_n values stabilize the dimeric protein form; thus, the dissociation process occurs at higher temperatures, whereas the unfolding process is not altered.

3.1.3. Effect of the Enthalpy of Oligomerization on Simulated Calorimetric Profiles. The sign of the oligomerization enthalpy has a crucial influence on the unfolding mechanism of an oligomeric protein system. With a dimeric protein, one can obtain a biphasic endotherm either with an exothermic or an endothermic dimerization process (Figure 2A,C).

In Figure 2 are also shown the energetic contributions to the dimerization/dissociation and unfolding process deconvoluted from the global calorimetric profile. From the information of the contributions and from the species profiles (Figure 2B,D), it is possible to understand the mechanisms of both global reactions. The protein system with a negative dimerization enthalpy value ($\Delta H_n^\circ < 0$) is, mainly, in the native dimeric form at low temperatures. As temperature increases, the dimer dissociates into the native monomer, and this phenomenon is observed as the first heat absorption peak. Then, at higher temperatures, the unfolding of the native monomeric protein produces the second endothermic contribution to the thermogram. The global reaction can be represented by eq V. The protein system with an endothermic dimerization process ($\Delta H_n^\circ > 0$) is, mainly, in the monomeric native state at the beginning of the endotherm. The increase in temperature induces the dimerization of the native monomers, as it is expected for an endothermic dimerization event, and this is observed as the first calorimetric transition. At higher temperatures, the dimer unfolds concomitantly with the dissociation process. The dissociation of the dimer occurs with the release of the heat which has been previously used to form the dimer. Thus, the dissociation contribution is observed as an exothermic peak. The unfolding contribution is an endothermic peak; therefore, the global transition is the sum of both contributions. The global reaction can be represented by the following mechanism:

$$2N \rightleftharpoons N_2 \rightleftharpoons 2D \qquad (VI)$$

The model allows the possibility of recognizing the unfolding mechanism of an oligomeric protein system. If a calorimetric experiment obtained with a dimeric protein system is biphasic, how could the mechanism undergone by the experimental reaction be deducted? The model predicts that the cases presented in Figure 2 can be solved with calorimetric experiments by changing the total protein concentration. Figure 3 shows the simulations for the two situations increasing C. The simulated calorimetric profiles of the protein system that has negative dimerization enthalpy (panel A) have a first transition which accounts for the dissociation of the dimer, and it occurs at higher temperatures when C is increased. The second transition is the unfolding of the native monomers, and this process is independent of C because its T_m value remains constant when total protein concentration is changed. The protein system that has positive dimerization enthalpy behaves in a very different way when C is changed. On the one hand, the T_m value of the first transition, which represents the association of two native monomers to form a native dimer, diminishes as C is

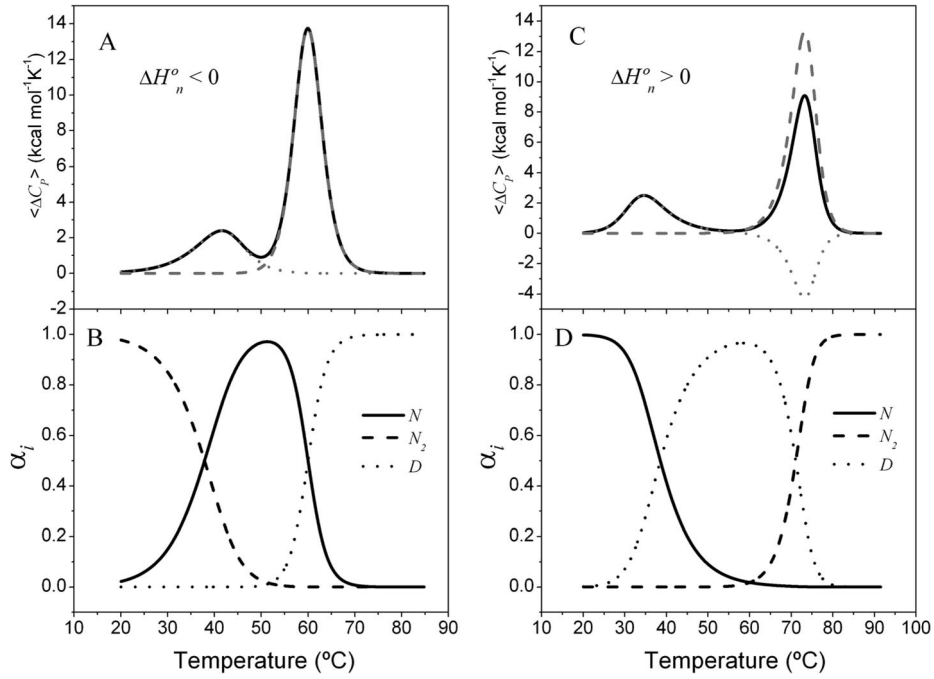

Figure 2. Effect of the enthalpy of oligomerization on simulated calorimetric profiles. (A) Exothermic dimerization enthalpy value; total heat capacity trace (solid line); calorimetric component from the dimerization process (dotted line); calorimetric component from the unfolding process (dashed line). Same simulation parameters as in Figure 1 except for $C = 1 \times 10^{-5}$ M, $K_n = 1 \times 10^8$ M^{-1}. (B) Species temperature-dependence profiles. (C) Endothermic dimerization enthalpy value; total heat capacity trace (solid line); calorimetric component from the association/dissociation process (dotted line); calorimetric component from the unfolding process (dashed line). Same simulation as in Panel A except for $\Delta H_n = 70$ kcal mol^{-1} of dimer, $T_n = 45$ °C, $K_n = 1 \times 10^6$ M^{-1}. (D) Species temperature-dependence profiles.

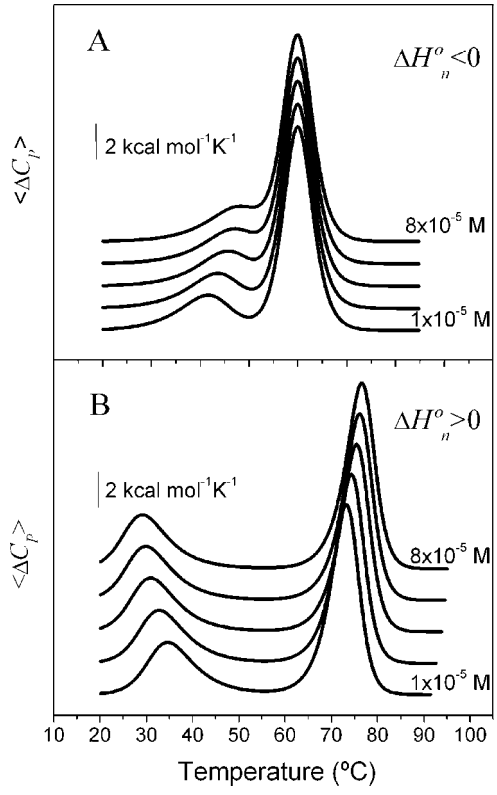

Figure 3. Total protein concentration effect on the stability of a protein with an exothermic dimerization process (A) and endothermic dimerization process (B). The simulation parameters in Panel A are the same as those employed in Figure 2A, and the simulation parameters in Panel B are the same as those employed in Figure 2C, except for $C = 1 \times 10^{-5}$–8×10^{-5} M.

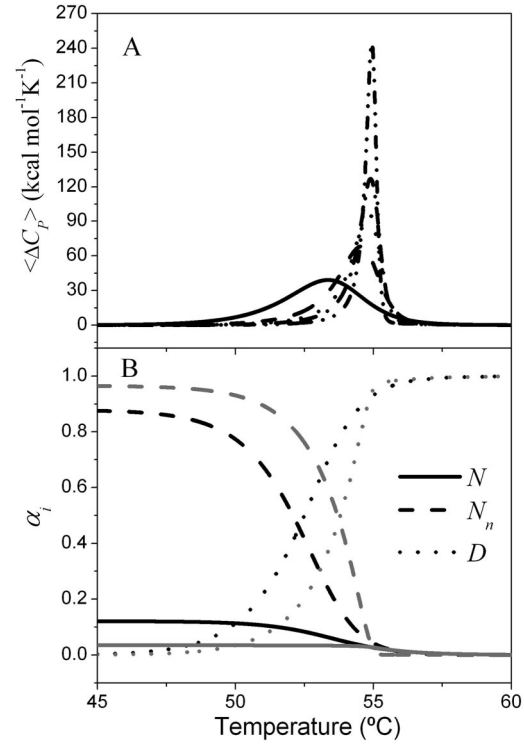

Figure 4. Comparison of calorimetric simulations with different oligomerization numbers. (A) Calorimetric profiles with $n = 2$ (solid line), 4 (dashed line), 6 (dotted line), 8 (dashed line), 16 (dashed-double-dotted line). (B) Species temperature-dependence profiles with $n = 2$ (black lines) and $n = 16$ (gray lines). Simulation parameters: $C = 3 \times 10^{-5}$ M, $T_d = 50$ °C, $\Delta H_d = 150$ kcal mol^{-1}, $\Delta C_P = 0$ kcal mol^{-1} K^{-1}, $K_n = 1 \times 10^6$ M^{-1}, $\Delta H_n = 0$ kcal mol^{-1}, $\Delta C_{Pn} = 0$ kcal mol^{-1} K^{-1}.

decreased. On the other hand, the T_m value of the second transition is higher when C is increased. This transition involves the dissociation and unfolding of the dimer. It is noteworthy that whenever there is a reaction with a change in the

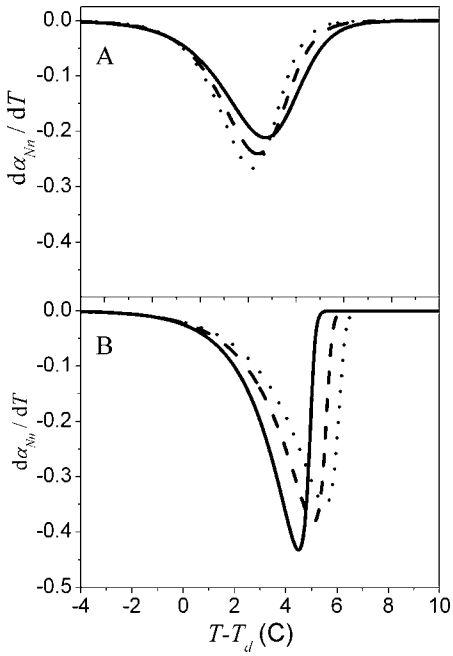

Figure 5. First derivative respect to temperature of the oligomer concentration profiles simulated with different T_D values. (A) $n = 2$, T_D =50 °C (solid line), T_D =30 °C (dashed line), T_D =15 °C (dotted line). (B) $n = 16$, $T_D = 50$ °C (solid line), $T_D = 70$ °C (dashed line), $T_D = 85$ °C (dotted line). Other simulation parameters are the same as those in Figure 4.

molecularity ($n\mathrm{N} \rightleftharpoons \mathrm{N}_n$), the T_m value of the calorimetric transition will be *C*-dependent.

3.2. Results Obtained with Model A for a *n*-Meric Protein. ***3.2.1. Comparison of Calorimetric Simulations with Different Oligomerization Numbers.*** In order to compare protein systems with different oligomerization numbers, the association constant must be normalized. The normalization procedure used in this section assumes the same free energy for the association of each monomer at the reference temperature. This procedure can be represented by the following scheme:

$$\begin{aligned} \mathrm{N} + \mathrm{N} &\rightleftharpoons \mathrm{N}_2 \Delta G_2 \\ &\vdots \\ \mathrm{N}_{n-1} + \mathrm{N} &\rightleftharpoons \mathrm{N}_n \Delta G_n = (n-1)\Delta G_2 \end{aligned} \qquad \text{(VII)}$$

This means that the temperature-dependent oligomerization constant should be $K_n(T) = (K_2(T))^n$.

In Figure 4 are presented calorimetric profiles of protein systems with different oligomerization numbers (n) (Panel A) and species profiles (Panel B) for $n = 2-16$. The systems with larger n have a higher proportion of total protein in the oligomeric state, as it is noticeable in the species-profile graph; therefore, the protein systems are more stable and unfold at higher temperatures.

It is interesting to observe that the calorimetric traces are also more cooperative and asymmetric when the system has larger n. It is important to take into account that it is not possible to have intermediates of oligomerization with this model; thus, cooperativity is only sensitive to the proportion of total protein concentration in the oligomeric state. The cooperativity of the unfolding process increases because the unfolding of one molecule of native monomer induces, for instance, the dissociation of an oligomer of $n = 16$ with the release of 16 protein monomers in the native state. This event has the consequence of shifting the unfolding equilibrium toward the unfolded state, increasing the cooperativity of the unfolding reaction, whereas the dissociation of a dimer releases only two protein monomers in the native state with a minor effect on the unfolding process. The asymmetry of the endotherms can be rationalized in the following way: the stability of the native monomer depends on the value of the reference unfolding temperature, T_D; if the oligomer dissociation takes place at a higher temperature than the T_D value, the native monomers released are thermodynamically unstable, and they unfold in a narrower temperature interval. Then, the side of the calorimetric profile that is further away from the T_D value progress more abruptly than the side that is nearer. In order to have a better understanding of how the intrinsic stability of the monomeric native protein affects the cooperativity and peak asymmetry of the simulated thermograms, we made simulations of a dimeric ($n = 2$) and a hexadecameric ($n = 16$) protein with different T_D values. Then, from the oligomer concentration profiles, we plotted the first derivative respect to temperature and compared them in Figure 5.

It is evident from the curves that, as the stability of the monomeric species is lowered, the dissociation of the oligomeric species becomes more cooperative. The thermodynamic explanation is that a positive unfolding enthalpy value implies that, at lower temperatures, the dependence of the unfolding constant, $K_D(T)$, with temperature is more abrupt, causing a transition with a higher degree of cooperativity. The effect on the oligomer dissociation reaction can be explained only on the basis of the coupled equilibrium theory.

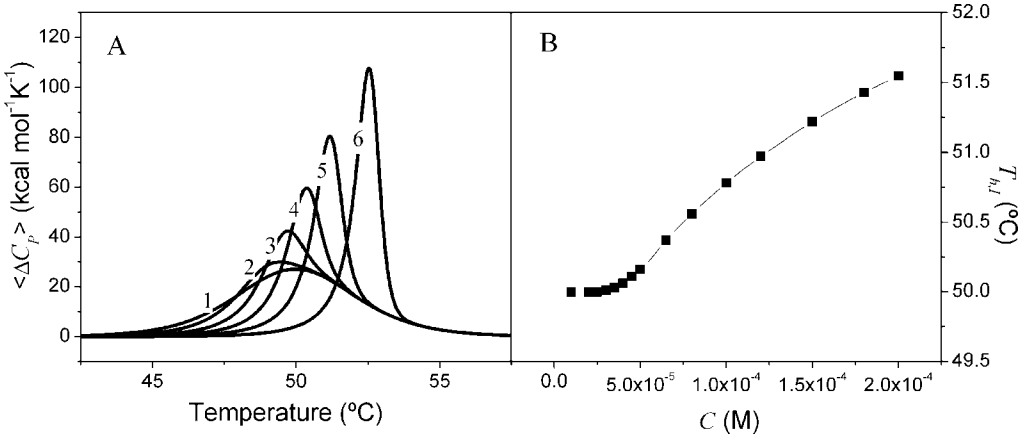

Figure 6. Stabilization of an octameric protein by increasing the total protein concentration. (A) Calorimetric simulation the following *C* values: (1) 8.0×10^{-6} M, (2) 2.5×10^{-5} M, (3) 3.5×10^{-5} M, (4) 5.0×10^{-5} M, (5) 8×10^{-5} M, (6) 2×10^{-4} M. (B) Total protein concentration dependence of the T_{hI} values. Simulation parameters: $n = 8$, $T_D = 50$ °C, ΔH_D =150 kcal mol^{-1}, $\Delta C_P = 0$ kcal mol^{-1} K^{-1}, $K_n = 2.5 \times 10^4$ M^{-1}, $T_n = 25$ °C, $\Delta H_n = 0$ kcal mol^{-1}, $\Delta C_{Pn} = 0$ kcal mol^{-1} K^{-1}.

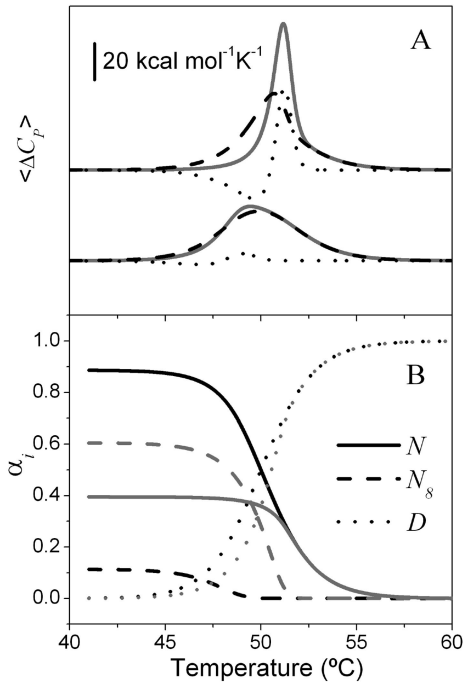

Figure 7. Influence of total protein concentration on endotherm-trace shapes. (A) Simulated calorimetric traces (2) and (5) from Figure 6 and their deconvolution of the heat capacity according to eq 16, (solid line) global thermogram, (dashed line) deconvolution of the first term from eq 16, (dotted line) deconvolution of the second term from eq 16. (B) α dependences on temperature, in gray for (2) and in black for (5).

3.2.2. Effect of Changing Total Protein Concentration on Simulated Calorimetric Profiles for a Protein Octamer. In general, the increment of total protein concentration stabilizes the oligomeric species and, as a consequence, the protein system is stabilized, which means that the unfolding process occurs at higher temperatures. We simulated calorimetric profiles for a protein octamer when C is increased from 8×10^{-6} M to 2×10^{-4} M, and some representative traces are shown in Figure 6A.

At $C = 8 \times 10^{-6}$ M, the majority of the protein is in the monomeric state; thus, the endotherm is almost symmetric around the T_D value. When C is raised, there seems to be a decrease in the protein stability for the first thermograms, but at higher C values, there is evident protein stabilization as the temperatures of the maximum of the transition peak, T_m, are quite larger than T_D. However, the T_{hI}, which is the temperature of half-completion of the reaction I, rises monotonically with C (Figure 6B), meaning that protein stability does not diminish at low C values. The calorimetric profiles simulated at low C values are biphasic, although there is no enthalpic contribution from the process of oligomerization (see Figure 6A, traces 2 and 3). The reason why these endotherms show this behavior can be answered with a deeper analysis of the enthalpy expression. Equation 8 can be rearranged as follows when ΔH_n equals zero:

$$H - H_N = \Delta H_D \alpha_D - \Delta H_D \frac{(n-1)\alpha_D \alpha_{Nn}}{1 + (n-1)\alpha_{Nn}} \qquad (16)$$

From this expression, it can be observed that the unfolding enthalpy can be separated in a contribution given only by the fraction of protein in the unfolded state, α_D, and another term which is negative and becomes significant only at temperatures where α_D and the fraction of total protein in the oligomeric state, α_{Nn}, have similar values ($\alpha_D \approx \alpha_{Nn} \neq 0$). Figure 7A shows two simulated calorimetric profiles from Figure 6A, at low and high C, and their deconvolution of the heat capacity according to eq 16. Figure 7B shows the species evolution with temperature.

In both cases, with low and high C, there is a contribution from the second term of eq 16 to the heat capacity profile, but it has more influence in the endotherm shape at high protein concentration, which is not biphasic because the dissociation and unfolding processes occur in a narrow temperature interval. On the contrary, at low C, the second term is more visible, producing the biphasic shape as the dissociation of the octamer occurs separately enough from the monomer unfolding process (Figure 7A,B).

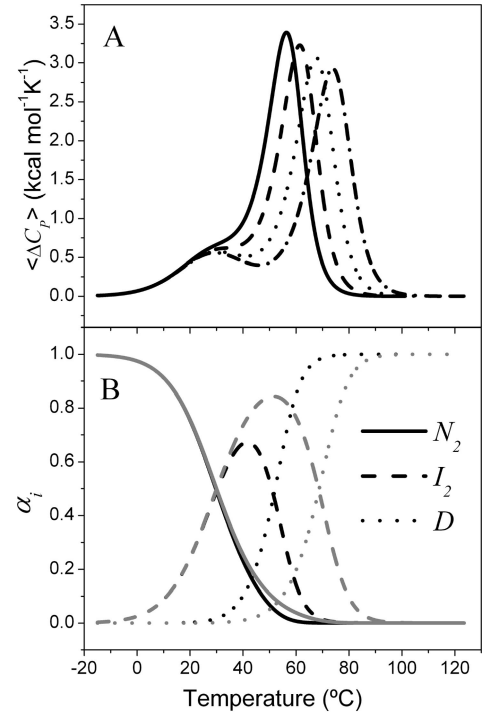

Figure 8. Calorimetric simulations obtained with model B for a dimeric protein with different C values. (A) (solid line) 1×10^{-6} M, (dashed line) 4×10^{-6} M, (dotted line) 2×10^{-5} M, (dashed-dotted line) 1×10^{-4} M. (B) α dependences on temperature for the lowest (black line) and the highest (gray line) C values. Simulation parameters: $n = 2$, $T_{ID} = 60$ °C, $\Delta H_{ID} = 80$ kcal mol^{-1}, $\Delta C_{PID} = 0$ kcal mol^{-1} K^{-1}, $K_{In} = 1$, $T_{In} = 30$ °C, $\Delta H_{In} = -20$ kcal mol^{-1}, $\Delta C_{PIn} = 0$ kcal mol^{-1} K^{-1}.

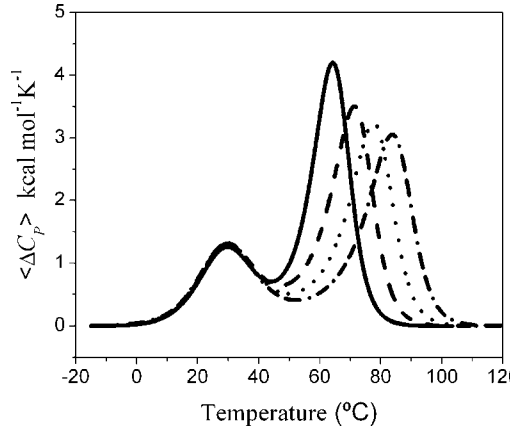

Figure 9. Comparison of calorimetric simulations with different oligomerization numbers obtained with model B. (solid line) $n = 2$, (dashed line) $n = 4$, (dotted line) $n = 6$, (dashed-dotted line) $n = 8$. Simulation parameters: $C = 5 \times 10^{-5}$ M, $T_{ID} = 60$ °C, $\Delta H_{ID} = 70$ kcal mol^{-1}, $\Delta C_{PID} = 0$ kcal mol^{-1} K^{-1}; $K_{In} = 1$, $T_{In} = 30$ °C, $\Delta H_{In} = -30$ kcal mol^{-1}, $\Delta C_{PIn} = 0$ kcal mol^{-1} K^{-1}.

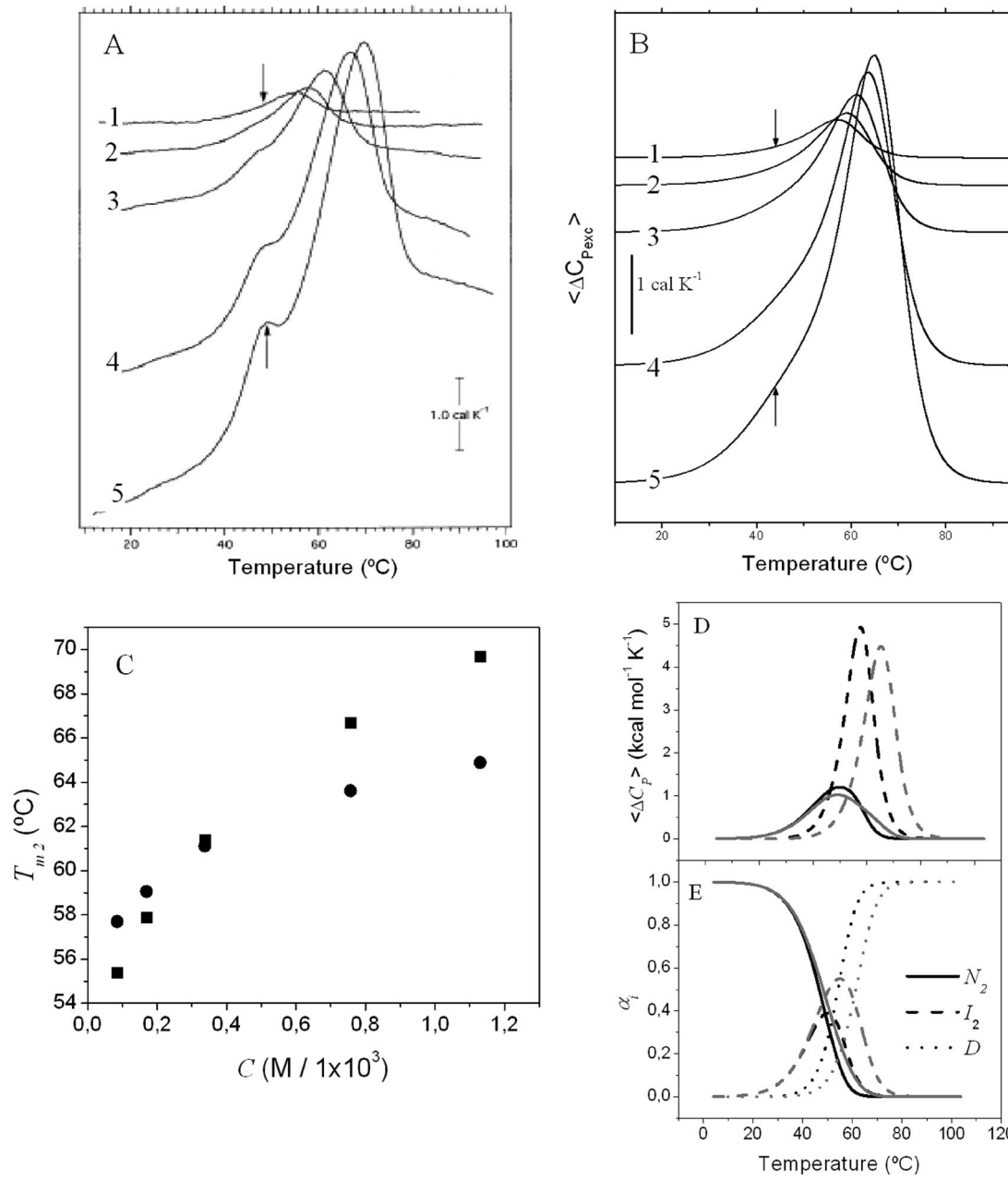

Figure 10. Comparison of the concentration dependence of DSC experimental curves of M103L Subtilisin Inhibitor from *Streptomyces*[7] (A) with calorimetric traces simulated with model B (B). In both cases, the endotherms are not normalized with protein concentration. *C* values: (1) 0.85×10^{-4} M, (2) 1.7×10^{-4} M, (3) 3.4×10^{-4} M, (4) 7.6×10^{-4} M, (5) 11.3×10^{-4} M. (C) Temperature of the maximum of the transition peak, T_m, as a function of *C*, from the experimental curves (■) and from the simulated curves (●). (D) Deconvolution of the conformational transition (solid line) and of the unfolding transition (dashed line), normalized by total protein concentration, and α-temperature profiles (E), for protein concentration (1) in black and (5) in gray. Simulation parameters: $n = 2$, $T_{1n} = 49.1$ °C, $\Delta H_{1n} = 28$ kcal mol^{-1}, $\Delta H_{ID} = 71.3$ kcal mol^{-1}, $\Delta C_{P1n} = 0$ kcal mol^{-1} K^{-1}, $\Delta C_{PID} = 0$ kcal mol^{-1} K^{-1}. Panel A reprinted with permission from ref 7, Copyright (1995) Elsevier.

3.3. Results Obtained with Model B. ***3.3.1. Effect of Changing Total Protein Concentration on Simulated Calorimetric Profiles.*** The reactions considered in model B are the conformational change of an oligomeric protein in its native state into an intermediate oligomeric state coupled with the unfolding of the intermediate state into the monomeric unfolded units. The effect of rising total protein concentration on biphasic endotherms simulated with model B is shown in Figure 8A.

The first transition is not sensitive to this change, whereas the T_m of the second transition increases progressively with *C*. According to the concentration profiles (Figure 8B), the first transition accounts for the conformational change between the N_n state and the I_n, and this process is *C*-independent because there is no change in the oligomerization state. The second transition is the heat uptake for the unfolding and dissociation of the intermediate state, and this change in the protein molecularity causes the observed T_m total protein concentration dependence. The oligomeric species are more stable when *C* is increased, and they unfold at higher temperatures. Unlike in model A, in this model, the association/dissociation process is not independent, meaning that the parameters of oligomerization, except *n*, cannot be independently modified. As a consequence, the effects produced by changes in the protein molecularity are less understood than for model A.

3.3.2. Comparison of Calorimetric Simulations with Different Oligomerization Numbers. Model B considers that the relevant thermodynamic states are the native protein oligomer, a conformational intermediate state, which is also oligomeric, and the unfolded protein in the monomeric state. The energy of protein association is implicitly present, stabilizing the native state. Then, it is thermodynamically expected that proteins with higher oligomerization number (n) will be more stable. In order to compare the stability of proteins with different oligomerization numbers, it was necessary to normalize the energy of the association/dissociation process. However, this normalization could not be done in a straightforward manner, as it was done for model A (see Section 3.2.2), because there is no explicit equilibrium of association/dissociation in model B; the oligomer dissociates and unfolds in a single step. Thus, the equilibrium constant of reaction III, $K_{ID}(T)$, was normalized with a pre-exponential factor for which, at the temperature of half-completion (T_{hIII}), the extent of the reaction is 0.5 (see Appendix II).

$$K_{ID}(T_{hIII}) = n\left(\frac{CK_{In}(T_{hIII})}{1+2K_{In}(T_{hIII})}\right)^{(n-1)} \qquad (17)$$

The simulated DSC traces, normalized with eq 17, for n values between 2 and 8, are shown in Figure 9. These results confirm that proteins with higher oligomeric states are more stable as the T_m value for the unfolding transition increases with higher n values.

3.4. Comparison between Experimental Results and Simulations Obtained with Model B. Some of the tendencies observed in the previous sections can reproduce results obtained from DSC experiments with oligomeric proteins. For instance, we were able to simulate DSC traces at different C values reproducing the C dependence of the M103L *Streptomyces* subtilisin inhibitor.[7] The wild type is a dimeric protein in the native state which unfolds in a single step. However, Tamura and Sturtevant[7] introduced a single mutation in the dimer interface, M103L, and the DSC traces of this mutant did not fit a single-step transition anymore. The authors proposed that an unfolding intermediate state should be significantly present during the process. They confirmed this hypothesis and proposed a mechanism performing calorimetric curves at different total protein concentrations of the mutant of the inhibitor of subtilisin (Figure 10A). At high values of total protein concentration (profiles (3), (4), and (5) from the graph), it is evident that the denaturation has two separated transitions. The first transition has its maximum value of heat capacity always at the same temperature, T_{m1}, independently from C, which means that in the reaction represented by the first transition, there is no change in the state of protein oligomerization. On the contrary, in the second transition, the final state, the unfolded state, should have a lower molecularity from the intermediate state as the peak moves to higher temperatures as C is increased. On the basis of this analysis, the authors proposed the following mechanism for the unfolding of the mutant M103L of subtilisin inhibitor:

$$N_2 \rightleftharpoons I_2 \rightleftharpoons 2D \qquad (VIII)$$

Then, on the basis of this scheme, they fitted the DSC curve of M103L at 1.95 mg mL^{-1} (curve 2) with a semiempiric model and obtained the thermodynamic parameters. By introducing this parameters in our model B and simulating DSC profiles at the same total concentration values as those in the experiment of M103L, we were successful to reproduce the tendency observed by Tamura and Sturtevant[7] (Figure 10BB), which means that the first transition of the simulated traces is independent of total protein concentration, and the second transition shifts toward higher temperatures as total protein concentration is increased. The peak temperatures for the second peak, T_{m2}, obtained from the experimental and simulated curves are plotted in Figure 10CC. Regarding to this comparison some considerations should be made. First, the simulations do not intend to emulate the exact shape of the experimental DSC traces, but to reproduce the general behavior observed with changes in C. Second, the theoretical curves represent only the excess heat capacity due to the cited work does not inform the ΔC_Pvalues. In fact, they recognize that the curve-fittings were not successful for concentrations above 4 mg mL^{-1}. They point out that the anomalously large values of apparentΔC_P that might come from intermolecular interaction are due to the high concentration. This may be the reason why at high concentrations exists more divergence between the T_{m2} obtained from the experimental and simulated DSC traces (Figure 10C). Finally, it is important to notice that the simulations allow the possibility to do the deconvolution of the main transition and, therefore, get information about the shape of the contributing transitions. In Figure 10D,E are shown the deconvoluted transitions from the simulated curves and the species profiles, respectively, at the lowest and the highest protein concentration. Further information can be obtained from thess outputs such as, for example, that at the lowest protein concentration, the shape of the first transition is not Gaussian, and the reason can be the overlapping with the unfolding reaction displacing the equilibrium.

Conclusions

Oligomeric proteins are complex systems, especially if they have more than two units. Therefore, the rationalization of their thermodynamic behavior is usually difficult to achieve, and the experimental results are hardly well fitted. We propose these general thermodynamic models as robust tools to explore and predict the thermal response of the association and unfolding parameters of oligomeric proteins. The simulation results obtained are in good agreement with the calorimetric results obtained by Tamura Sturtevant.[7]

Acknowledgment. S.A.D. and G.D.F. are Career members of Consejo Nacional de Investigaciones Científicas y Tecnológicas (CONICET). I.B. thanks CONICET for the fellowships granted. This work was supported by grants from CONICET, Secretaría de Ciencia y Tecnología (SECyT-UNC) and Foncyt.

Appendix I

In order to solve eq 7, it is necessary to define$\partial Q/\partial T|_C$, but Q is a function of [D]. Therefore, the following generic operator is defined:[9]

$$\left.\frac{\partial}{\partial T}\right|_{[D]} = \left.\frac{\partial T}{\partial T}\right|_{[D]}\left.\frac{\partial}{\partial T}\right|_C + \left.\frac{\partial C}{\partial T}\right|_{[D]}\left.\frac{\partial}{\partial C}\right|_T \qquad (A1)$$

Also,

$$\left.\frac{\partial}{\partial C}\right|_T = \left.\frac{\partial [D]}{\partial C}\right|_T\left.\frac{\partial}{\partial [D]}\right|_T = \left(\left.\frac{\partial C}{\partial [D]}\right|_T\right)^{-1}\left.\frac{\partial}{\partial [D]}\right|_T = \frac{Q_D}{Q_N(1+Q_D)+nQ_{Nn}}\left.\frac{\partial}{\partial [D]}\right|_T \qquad (A2)$$

Therefore, eq A1 turns to be

$$\left.\frac{\partial}{\partial T}\right|_{[D]} = \left.\frac{\partial}{\partial T}\right|_{C} - \frac{[D]}{k_B T^2}[\Delta H_D + Q_{Nn}(n\Delta H_D - \Delta H_n)] \times \frac{1}{1 + Q_D + nQ_{Nn}} \left.\frac{\partial}{\partial [D]}\right|_{T} \quad \text{(A3)}$$

where ΔH_D and ΔH_n are the enthalpies, at the reference temperature, for reactions I and II, respectively. From this expression, it is possible to obtain the partial derivative of the relative partition function, Q, with respect to temperature for total protein concentration constant:

$$\left.\frac{\partial Q}{\partial T}\right|_{C} = \frac{1}{k_B T^2}\left\{K_D \Delta H_D + Q_{Nn}[(1-n)\Delta H_D + \Delta H_n] + \Delta H_D + Q_{Nn}(n\Delta H_D - \Delta H_n)\left(\frac{(n-1)Q_{Nn}}{1 + Q_D + nQ_{Nn}}\right)\right\} \quad \text{(A4)}$$

Then, by employing eqs 7 and A4, the analytical expression for the mean enthalpy of the protein system relative to the reference state was obtained.

A similar procedure was employed to solve the equations used in model B.

Appendix II

In order to obtain eq 17, it is necessary to define that, at the temperature of half-completion (T_{hIII}),

$$n[I_n] = [D] \quad \text{(A5)}$$

$$n[I_n] = \frac{C - n[N_n]}{2} \quad \text{(A6)}$$

$$2n[I_n] = C - \frac{n[I_n]}{K_{In}(T_{hIII})} \quad \text{(A7)}$$

$$[I_n] = \frac{C}{n\{2 + [K_{In}(T_{hIII})]^{-1}\}} \quad \text{(A8)}$$

$$[D] = \frac{C}{\{2 + [K_{In}(T_{hIII})]^{-1}\}} \quad \text{(A9)}$$

$$K_{ID}(T_{hIII}) = \frac{\left(\frac{C}{\{2 + [K_{In}(T_{hIII})]^{-1}\}}\right)^n}{\frac{C}{n\{2 + [K_{In}(T_{hIII})]^{-1}\}}} \quad \text{(A10)}$$

$$K_{ID}(T_{hIII}) = n\left[\frac{CK_{In}(T_{hIII})}{1 + 2K_{In}(T_{hIII})}\right]^{(n-1)} \quad \text{(A11)}$$

Supporting Information Available: The consequences of modifying the equilibrium constant value of the dimerization process on protein stability with K_n are shown in Figure S1. This material is available free of charge via the Internet at http://pubs.acs.org.

References and Notes

(1) Zomosa-Signoret, V.; Hernandez-Alcantara, G.; Reyes-Vivas, H.; Martinez-Martinez, E.; Garza-Ramos, G.; Perez-Montfort, R.; Tuena, D. G.-P.; Gomez-Puyou, A. Control of the reactivation kinetics of homodimeric triosephosphate isomerase from unfolded monomers. *Biochemistry* **2003**, *42* (11), 3311–3318.

(2) Katz, R. A.; Skalka, A. M. The retroviral enzymes. *Annu. Rev. Biochem.* **1994**, *63*, 133–173.

(3) Sagar, G. D.; Gereben, B.; Callebaut, I.; Mornon, J. P.; Zeold, A.; da Silva, W. S.; Luongo, C.; Dentice, M.; Tente, S. M.; Freitas, B. C.; Harney, J. W.; Zavacki, A. M.; Bianco, A. C. Ubiquitination-induced conformational change within the deiodinase dimer is a switch regulating enzyme activity. *Mol. Cell. Biol.* **2007**, *27* (13), 4774–4783.

(4) Frieden, C. Protein aggregation processes: In search of the mechanism. *Protein Sci.* **2007**, *16* (11), 2334–2344.

(5) Takahashi, Y.; Okamoto, Y.; Popiel, H. A.; Fujikake, N.; Toda, T.; Kinjo, M.; Nagai, Y. Detection of polyglutamine protein oligomers in cells by fluorescence correlation spectroscopy. *J. Biol. Chem.* **2007**, *282* (33), 24039–24048.

(6) Takahashi, K.; Sturtevant, J. M. Thermal denaturation of streptomyces subtilisin inhibitor, subtilisin BPN′, and the inhibitor-subtilisin complex. *Biochemistry* **1981**, *20* (21), 6185–6190.

(7) Tamura, A.; Sturtevant, J. M. A thermodynamic study of mutant forms of Streptomyces subtilisin inhibitor. I. Hydrophobic replacements at the position of Met103. *J. Mol. Biol.* **1995**, *249* (3), 625–635.

(8) Tamura, A.; Kojima, S.; Miura, K.; Sturtevant, J. M. A thermodynamic study of mutant forms of Streptomyces subtilisin inhibitor. II. Replacements at the interface of dimer formation, Val13. *J. Mol. Biol.* **1995**, *249* (3), 636–645.

(9) Rösgen, J.a.; Hinz, J. Statistical thermodynamic treatment of conformational transitions of monomeric and oligomeric proteins. *Phys. Chem. Chem. Phys.* **1999**, *1*, 2327–2333.

(10) Freire, E.; Biltonen, R. Statistical mechanical deconvolution of thermal transitions in macromolecules. I. Theory and application to homogeneous systems. *Biopolymers* **1978**, *17*, 463–479.

JP804465C

Supporting Information Available

The consequences of modifying the equilibrium constant value of the dimerization process on protein stability with K_n are shown in Figure S1. This material is available free of charge via the Internet at http://pubs.acs.org.

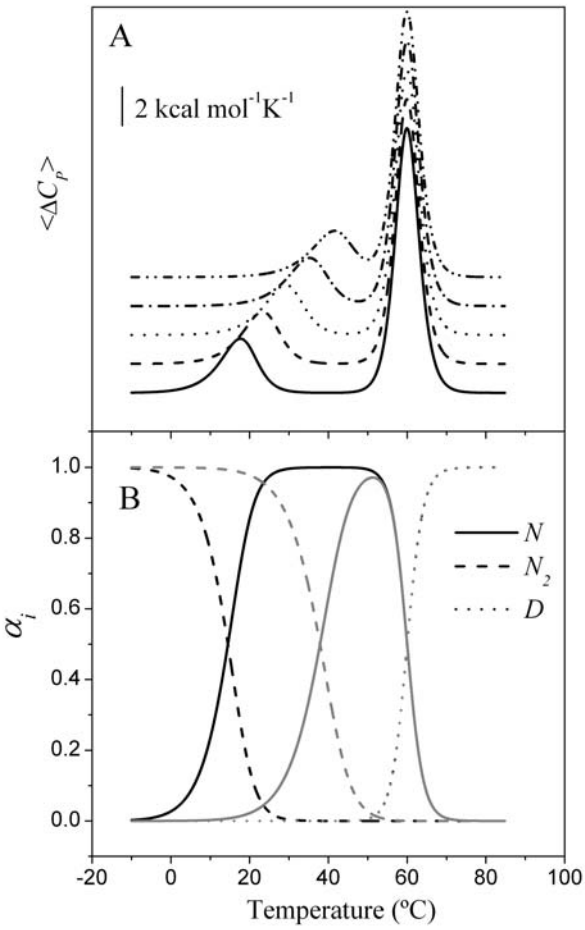

Figure S1

Figure S1: Effect the dimerization equilibrium constant value of on the stability of a dimeric protein complex. (A) Simulated thermograms changing the equilibrium constant value K_n = (□) 1×10^3 M^{-1}, (□) 1×10^4 M^{-1}, (□)1×10^5 M^{-1}, (□) 1×10^6 M^{-1}, (□) 1×10^7 M^{-1}. (B) species temperature dependence profiles with K_n =1×10^3 M^{-1} in black lines and K_n =1×10^7 M^{-1} in gray lines.

Simulation parameters: n = 2, T_d = 60 ºC, ΔH_d =110 kcal mol^{-1}, ΔC_P = 0 kcal mol^{-1}K^{-1}, C=1×10^4 M, T_n=20 ºC, ΔH_n = −70 kcal mol^{-1}of dimer, ΔC_{Pn}= 0 kcal mol^{-1}K^{-1}.